Physics Letters B 757 (2016) 356–361

Contents lists available at ScienceDirect

Physics Letters B

www.elsevier.com/locate/physletb

Limit on the production of a new vector boson in $e^+e^- \to U\gamma$, $U \to \pi^+\pi^-$ with the KLOE experiment

The KLOE-2 Collaboration

A. Anastasi [e,d], D. Babusci [d], G. Bencivenni [d], M. Berlowski [v], C. Bloise [d], F. Bossi [d], P. Branchini [r], A. Budano [q,r], L. Caldeira Balkeståhl [u], B. Cao [u], F. Ceradini [q,r], P. Ciambrone [d], F. Curciarello [e,b,l,*], E. Czerwiński [c], G. D'Agostini [m,n], E. Danè [d], V. De Leo [r], E. De Lucia [d], A. De Santis [d], P. De Simone [d], A. Di Cicco [q,r], A. Di Domenico [m,n], R. Di Salvo [p], D. Domenici [d], A. D'Uffizi [d], A. Fantini [o,p], G. Felici [d], S. Fiore [s,n], A. Gajos [c], P. Gauzzi [m,n], G. Giardina [e,b], S. Giovannella [d], E. Graziani [r], F. Happacher [d], L. Heijkenskjöld [u], W. Ikegami Andersson [u], T. Johansson [u], D. Kamińska [c], W. Krzemien [v], A. Kupsc [u], S. Loffredo [q,r], G. Mandaglio [f,g,*], M. Martini [d,k], M. Mascolo [d], R. Messi [o,p], S. Miscetti [d], G. Morello [d], D. Moricciani [p], P. Moskal [c], A. Palladino [t], M. Papenbrock [u], A. Passeri [r], V. Patera [j,n], E. Perez del Rio [d], A. Ranieri [a], P. Santangelo [d], I. Sarra [d], M. Schioppa [h,i], M. Silarski [d], F. Sirghi [d], L. Tortora [r], G. Venanzoni [d], W. Wiślicki [v], M. Wolke [u]

[a] *INFN Sezione di Bari, Bari, Italy*
[b] *INFN Sezione di Catania, Catania, Italy*
[c] *Institute of Physics, Jagiellonian University, Cracow, Poland*
[d] *Laboratori Nazionali di Frascati dell'INFN, Frascati, Italy*
[e] *Dipartimento di Scienze Matematiche e Informatiche, Scienze Fisiche e Scienze della Terra dell'Università di Messina, Messina, Italy*
[f] *Dipartimento di Scienze Chimiche, Biologiche, Farmaceutiche ed Ambientali dell'Università di Messina, Messina, Italy*
[g] *INFN Gruppo Collegato di Messina, Messina, Italy*
[h] *Dipartimento di Fisica dell'Università della Calabria, Rende, Italy*
[i] *INFN Gruppo Collegato di Cosenza, Rende, Italy*
[j] *Dipartimento di Scienze di Base ed Applicate per l'Ingegneria dell'Università "Sapienza", Roma, Italy*
[k] *Dipartimento di Scienze e Tecnologie Applicate, Università "Guglielmo Marconi", Roma, Italy*
[l] *Novosibirsk State University, 630090 Novosibirsk, Russia*
[m] *Dipartimento di Fisica dell'Università "Sapienza", Roma, Italy*
[n] *INFN Sezione di Roma, Roma, Italy*
[o] *Dipartimento di Fisica dell'Università "Tor Vergata", Roma, Italy*
[p] *INFN Sezione di Roma Tor Vergata, Roma, Italy*
[q] *Dipartimento di Matematica e Fisica dell'Università "Roma Tre", Roma, Italy*
[r] *INFN Sezione di Roma Tre, Roma, Italy*
[s] *ENEA UTTMAT-IRR, Casaccia R.C., Roma, Italy*
[t] *Department of Physics, Boston University, Boston, USA*
[u] *Department of Physics and Astronomy, Uppsala University, Uppsala, Sweden*
[v] *National Centre for Nuclear Research, Warsaw, Poland*

ARTICLE INFO

Article history:
Received 18 March 2016
Received in revised form 6 April 2016
Accepted 7 April 2016
Available online 11 April 2016
Editor: L. Rolandi

ABSTRACT

The recent interest in a light gauge boson in the framework of an extra U(1) symmetry motivates searches in the mass range below 1 GeV. We present a search for such a particle, the dark photon, in $e^+e^- \to U\gamma$, $U \to \pi^+\pi^-$ based on 28 million $e^+e^- \to \pi^+\pi^-\gamma$ events collected at DAΦNE by the KLOE experiment. The $\pi^+\pi^-$ production by initial-state radiation compensates for a loss of sensitivity of previous KLOE $U \to e^+e^-$, $\mu^+\mu^-$ searches due to the small branching ratios in the ρ–ω resonance region. We found no evidence for a signal and set a limit at 90% CL on the mixing strength between the photon and the

* Corresponding authors.
E-mail addresses: fcurciarello@unime.it (F. Curciarello), gmandaglio@unime.it (G. Mandaglio).

http://dx.doi.org/10.1016/j.physletb.2016.04.019

Keywords:
Dark matter
Dark forces
Dark photon
U boson

dark photon, ε^2, in the U mass range between 527 and 987 MeV. Above 700 MeV this new limit is more stringent than previous ones.

1. Introduction

A new kind of matter, called dark matter (DM), which does not absorb or emit light, has been postulated since the early '30s of the past century [1] and its existence is now widely accepted [2]. However, its interpretation is still among the greatest and fascinating enigmas of Physics. The current paradigm assumes that the DM is a thermal relic from the Big Bang, accounting for about 24% of the total energy density of the Universe [2] and producing effects only through its gravitational interactions with large-scale cosmic structures. To include the DM in a particle theoretical framework, the Standard Model (SM) is usually complemented with many extensions [3–7] that attribute to the DM candidates also strong self interactions and weak-scale interactions with SM particles. Among the possible candidates, a Weakly Interacting Massive Particle (WIMP) aroused much interest since a particle with weak-scale annihilation cross section can account for the DM relic abundance estimated through the study of the cosmic microwave background [2]. The force carrier in WIMP annihilations could be a new gauge vector boson, known as U boson, dark photon, γ' or A′, with allowed decays into leptons and hadrons. Its assiduous worldwide search has been strongly motivated by the astrophysical evidence recently observed in many experiments [8–14] and by its possible positive one-loop contribution to the theoretical value of the muon magnetic moment anomaly [15], which could solve, partly or entirely, the well known 3.6 σ discrepancy with the experimental measurement [16].

In this paper we assume the simplest theoretical hypothesis according to which the dark sector consists of just one extra abelian gauge symmetry, U(1), with one gauge boson, the U boson, whose decays into invisible light dark matter are kinematically inaccessible. In this framework the dark photon would act like a virtual photon, with virtuality $q^2 = m_U^2$. It would couple to leptons and quarks with the same strength and would appear (its width being much smaller than the experimental mass resolution) as a narrow resonance in any process involving real or virtual photons. The coupling to the SM photon would occur by means of a vector portal mechanism [3], i.e. loops of heavy dark particles charged under both the SM and the dark force. The strength of the mixing with the photon is parametrized by a single factor $\varepsilon^2 = \alpha'/\alpha$ which is the ratio of the effective dark and SM photon couplings [3]. The size of the ε^2 parameter is expected to be very small (10^{-2}–10^{-8}) causing a suppression of the U boson production rate. The U boson decays into SM particles would happen through the same mixing operator, with the corresponding decay amplitude suppressed by an ε^2 factor, but are still expected to be detectable at high luminosity e^+e^- colliders [17–19].

KLOE has already searched for radiative U boson production in the $e^+e^- \to U\gamma$, $U \to e^+e^-$, $\mu^+\mu^-$ processes [20,21]. The leptonic channels are affected by a decrease in sensitivity in the ρ–ω region due to the dominant branching fraction into hadrons. For a virtual photon with $q^2 < 1$ GeV^2, the coupling to the charged pion is given by the product of the electric charge and the pion form factor, $e\,F_\pi(q^2)$. The effective coupling of the U boson to pions is thus predicted to be given by the product of the virtual photon coupling and the kinetic mixing parameter $\varepsilon^2\, e\, F_\pi(q^2)$ [19]. Being far from the $\pi^+\pi^-$ mass threshold (see Section 3) finite mass effects can be safely neglected. We thus searched for a short lived U boson decaying to $\pi^+\pi^-$ in a data sample corresponding to 1.93 fb^{-1} integrated luminosity, by looking for a resonant peak in the dipion invariant mass spectrum with initial-state radiation (ISR) $\pi^+\pi^-\gamma$ events.

2. The KLOE detector

The KLOE detector operates at DAΦNE, the Frascati ϕ-factory. DAΦNE is an e^+e^- collider usually operated at a center of mass energy $m_\phi \simeq 1.019$ GeV. Positron and electron beams collide at an angle of $\pi - 25$ mrad, producing ϕ mesons nearly at rest. The KLOE detector consists of a large cylindrical drift chamber (DC) [22], surrounded by a lead scintillating-fiber electromagnetic calorimeter (EMC) [23]. A superconducting coil around the EMC provides a 0.52 T magnetic field along the bisector of the colliding beams. The bisector is taken as the z axis of our coordinate system. The x axis is horizontal, pointing to the center of the collider rings and the y axis is vertical, directed upwards.

The EMC barrel and end-caps cover 98% of the solid angle. Calorimeter modules are read out at both ends by 4880 photomultipliers. Energy and time resolutions are $\sigma_E/E = 0.057/\sqrt{E(\text{GeV})}$ and $\sigma_t = 57$ ps$/\sqrt{E(\text{GeV})} \oplus 100$ ps, respectively. The drift chamber has only stereo wires and is 4 m in diameter, 3.3 m long. It is built out of carbon-fibers and operates with a low-Z gas mixture (helium with 10% isobutane). Spatial resolutions are $\sigma_{xy} \sim 150$ μm and $\sigma_z \sim 2$ mm. The momentum resolution for large angle tracks is $\sigma(p_\perp)/p_\perp \sim 0.4\%$. The trigger uses both EMC and DC information. Events used in this analysis are triggered by at least two energy deposits larger than 50 MeV in two sectors of the barrel calorimeter [24].

3. Event selection

We selected $\pi^+\pi^-\gamma$ candidates by requesting events with two oppositely-charged tracks emitted at large polar angles, $50° < \theta < 130°$, with the undetected ISR photon missing momentum pointing – according to the $\pi^+\pi^-\gamma$ kinematics – at small polar angles ($\theta < 15°$, $\theta > 165°$). The tracks were required to have the point of closest approach to the z axis within a cylinder of radius 8 cm and length 15 cm centered at the interaction point. In order to ensure good reconstruction and efficiency, we selected tracks with transverse and longitudinal momentum in the range $p_\perp > 160$ MeV or $p_\parallel > 90$ MeV, respectively.

Since the $\pi^+\pi^-\gamma$ cross section behavior as a function of the ISR photon polar angle is divergent ($\propto 1/\theta_\gamma^4$), the track and the photon acceptance selections make the final-state radiation (FSR) and the ϕ resonant processes relatively unimportant, leaving us with a high purity ISR sample and increasing our sensitivity to the $U \to \pi^+\pi^-$ decay [25].

The Monte Carlo simulation of the $M_{\pi\pi}$ spectrum was produced with the PHOKHARA event generator [26] with the Kühn–Santamaria (KS) [27] pion form factor parametrization and included a full description of the KLOE detector (GEANFI package [28]). The collected data were simulated including ϕ decays and leptonic processes $e^+e^- \to \ell^+\ell^-\gamma(\gamma)$, $\ell = e, \mu$. The main background contributions affecting the ISR $\pi^+\pi^-\gamma$ sample are the resonant $e^+e^- \to \phi \to \pi^+\pi^-\pi^0$ process and the ISR and FSR $e^+e^- \to \ell^+\ell^-\gamma(\gamma)$, $\ell = e, \mu$ processes (they will be defined as "residual

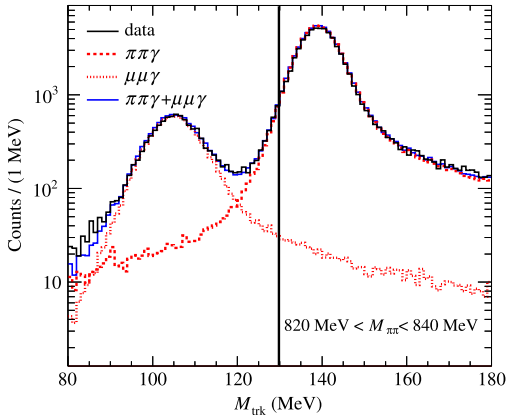

Fig. 1. Example of M_{trk} distributions for the $M_{\pi\pi} = 820$–840 MeV bin. Measured data are represented in black, simulated $\pi^+\pi^-\gamma$ and $\mu^+\mu^-\gamma$ in red. Simulated $\mu^+\mu^-\gamma + \pi^+\pi^-\gamma$ in blue. Events at the left of the vertical line are rejected. (For interpretation of the references to color in this figure legend, the reader is referred to the web version of this article.)

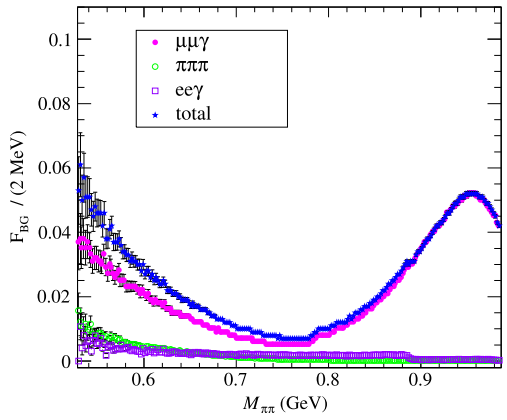

Fig. 2. Fractional backgrounds, normalized to the $\pi^+\pi^-\gamma$ contribution, from the $\pi^+\pi^-\pi^0$, $e^+e^-\gamma$, and $\mu^+\mu^-\gamma$ channels after all selection criteria.

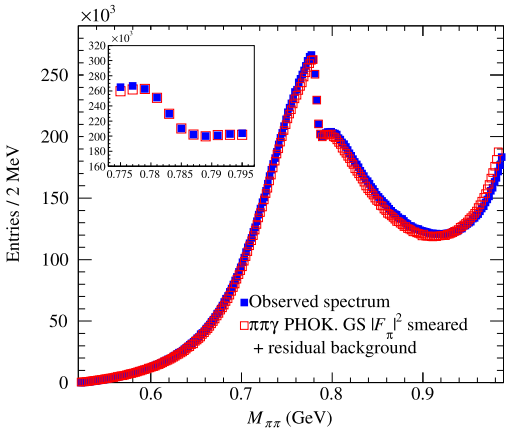

Fig. 3. Comparison of measured data (blue squares) and simulation performed with the Gounaris–Sakurai $|F_\pi|^2$ parametrization (red open squares) for the $M_{\pi\pi}$ invariant mass spectrum. The figure insert shows in detail the agreement achieved in the ρ–ω mixing region (779–791 MeV).

background" in the following). We reduced their contribution by applying kinematic cuts in the M_{trk}–$M^2_{\pi\pi}$ plane, as explained in Refs. [29,30]. $M^2_{\pi\pi}$ is the squared invariant mass of the two selected tracks in the pion mass hypothesis while M_{trk} is the mass of the charged particles associated to the tracks, computed in the equal mass hypothesis and assuming that the missing momentum of the event pertains to a single photon.[1] Distributions of the M_{trk} variable for data and simulation are shown in Fig. 1, where the $M_{trk} > 130$ MeV cut to discriminate muons from pions is also indicated.

A particle ID estimator (PID), $L_\pm$, defined for each track with associated energy released in EMC and based on a pseudo-likelihood function, uses calorimeter information (size and shape of the energy depositions and time of flight) to suppress radiative Bhabha scattering events [29–31].

Electrons deposit their energy mainly at the entrance of the calorimeter while muons and pions tend to have a deeper penetration in the EMC. Events with both tracks having $L_\pm < 0$ are identified as $e^+e^-\gamma$ events and rejected. The efficiency of this selection is larger than 99.95% as evaluated using measured data and simulated $\pi^+\pi^-\gamma$ samples.

After these selections, about 2.8×10^7 events are left in the measured data sample. We then applied the same analysis chain to the Monte Carlo simulated data: most of the selected sample consists of $\pi^+\pi^-\gamma$ events, with residual ISR $\ell^+\ell^-\gamma$, $\ell = e, \mu$ and $\phi \to \pi^+\pi^-\pi^0$. Fig. 2 shows the fractional components of the residual background, F_{BG}, individually for each contributing channel and their sum. The residual background rises up to about 6% at low invariant masses and to 5% above 0.9 GeV, decreasing to less than 1% in the resonance region, and it is dominated by $\mu\mu\gamma$ events in the whole invariant mass range.

A very good description of the ρ–ω interference region (see the insert of Fig. 3) was achieved by producing a dedicated sample using PHOKHARA as event generator with the Gounaris–Sakhurai (GS) pion form factor parametrization [32]. The generation process used properly smeared distributions in order to account for the dipion invariant mass resolution (1.4–1.8 MeV). In Fig. 3 the measured data spectrum is compared with the results of this simulation process, which includes the residual background.

[1] M_{trk} is computed from the measured momenta of the two particles $\vec{p}_\pm$ assuming they have the same mass: $\left(\sqrt{s} - \sqrt{|\vec{p}_+|^2 + M^2_{trk}} - \sqrt{|\vec{p}_-|^2 + M^2_{trk}}\right)^2 - \left(\vec{p}_+ + \vec{p}_-\right)^2 = M^2_\gamma = 0$.

4. Irreducible background parametrization and estimate

Except for the ρ–ω region, we estimated the irreducible background directly from data. For each U mass hypothesis the data are fitted in a $M_{\pi\pi}$ interval centered at M_U and 18–20 times wider than the $M_{\pi\pi}$ resolution $\sigma_{M_{\pi\pi}}$. The background is modeled by a monotonic function using Chebyshev polinomials up to the sixth order and is estimated using the sideband technique, by excluding from the fit the data in the region $\pm 3\sigma_{M_{\pi\pi}}$ around M_U [20]. The procedure is repeated in steps of 2 MeV in M_U.

Fits with the best reduced χ^2 are selected as histograms representing the background. For all used mass intervals, the distributions were found to be smooth, with no "wiggles" in any mass sub-range. An example of the fit procedure is reported in Fig. 4. Fig. 5 shows the distribution of the differences (pulls) between data and the fitted background normalized to the data statistical error. Also shown is a Gaussian fit of this distribution. The mean and width parameters of the Gaussian fit are around zero and one, respectively.

The region of ρ–ω interference is not smooth (see Fig. 3) and then not easy to be fitted with the sideband technique. We thus estimated the background in this region by using the PHOKHARA generator with smeared distributions, as explained in Section 3 and shown in Fig. 3 for the 779–791 MeV mass range.

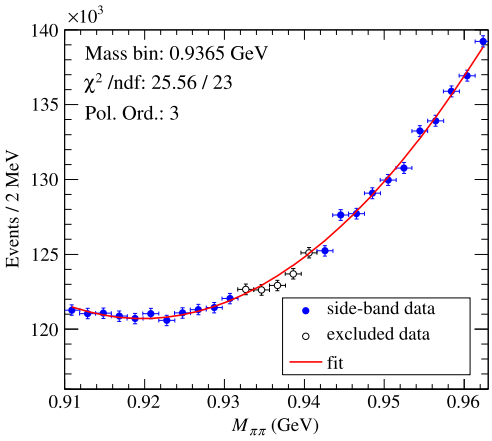

Fig. 4. Example of a Chebyshev polinomial sideband fit for the $M_U = 936$ MeV hypothesis.

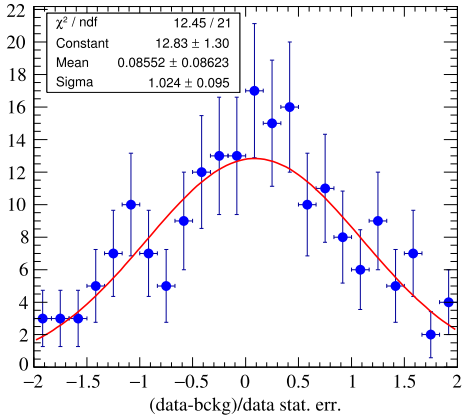

Fig. 5. Distribution of the differences (pulls) data-background normalized to the data statistical error (blue points) and relative Gaussian fit (red curve).

5. Systematic errors and efficiencies

The main systematic uncertainties affecting this analysis are related to the evaluation of the irreducible background. As two different procedures were used in different mass ranges, the estimate of the systematic error is accounted for two independent sources:

- systematic uncertainties due to the sideband fitting procedure;
- systematic uncertainties due to the evaluation of the background with the PHOKHARA generator and to the smearing procedure in the 779–791 MeV mass range.

The evaluation of the systematic uncertainties on the fitted background was performed by adding in quadrature, bin by bin, the contributions due to the errors of the fit and a systematic error due to the fit procedure. The first is obtained by propagating, for each fit interval, the corresponding errors of the fit parameters. The second is evaluated by varying the fit parameters by $\pm 1\sigma$ and computing the maximum difference between the standard fit and the fit derived by using the modified parameters. The systematic error is less than 1% in most of the mass range.

In the ρ–ω region the systematic error is computed by adding in quadrature the contributions due to the theoretical uncertainty of the Monte Carlo generator (0.5% [26]), the systematic error due to the residual background evaluation (0.3%, computed by changing the analysis cuts within the corresponding experimental resolutions), the contribution of the smearing procedure (0.8%, obtained by varying the applied smearing of $\pm 1\sigma$), and the systematic uncertainty on the luminosity (0.3% [26]). The resulting total systematic error is about 1%.

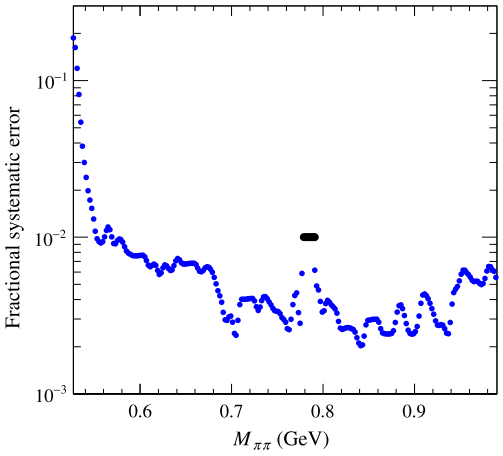

Fig. 6. Fractional systematic error on the estimated background. Blue points: errors from the sideband fit procedure; black points: errors estimated from the PHOKHARA Monte Carlo simulation for the ρ–ω interference region. (For interpretation of the references to color in this figure, the reader is referred to the web version of this article.)

Table 1
Summary of the systematic uncertainties affecting the $\pi^+\pi^-\gamma$ analysis.

Systematic source	Relative uncertainty (%)
M_{trk} cut	0.2
Acceptance	0.6–0.1 as $M_{\pi\pi}$ increases
Trigger	0.1
Tracking	0.3
Generator	0.5
Luminosity	0.3
PID	negligible
Total	0.9–0.7 as $M_{\pi\pi}$ increases

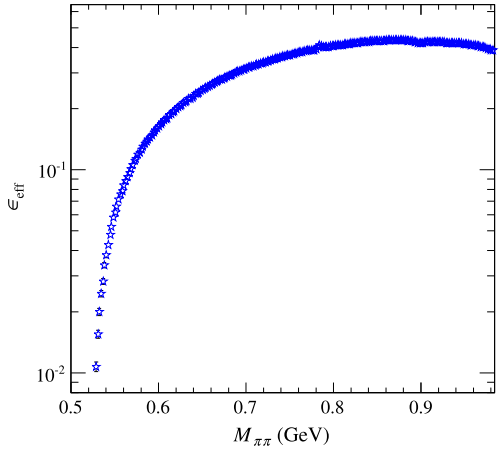

Fig. 7. Global analysis efficiency as a function of $M_{\pi\pi}$.

The total systematic uncertainty due to the background evaluation is shown in Fig. 6. The full list of the systematic effects taken into account is summarized in Table 1. They do not affect the irreducible background estimate performed with the sideband fitting technique, but partially contribute to the background estimate in the ρ–ω region (see above) and enter in the determination of the selection efficiency and the luminosity measurement. Finally, in Fig. 7 we show the global analysis efficiency as estimated with the full $\pi^+\pi^-\gamma$ simulation (PHOKHARA generator + GEANFI [28]).

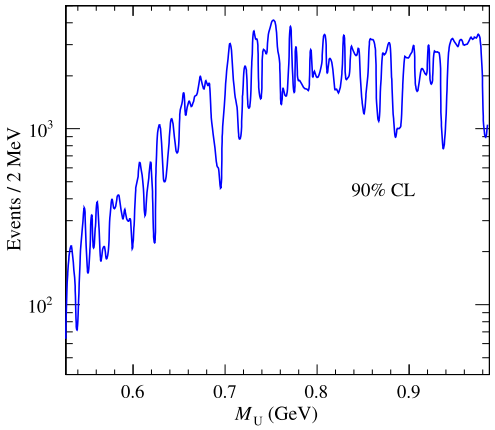

Fig. 8. Maximum number of U boson events excluded at 90% CL.

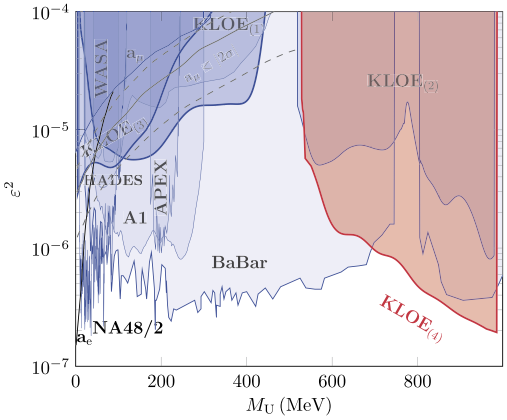

Fig. 9. 90% CL exclusion plot for ε^2 as a function of the U-boson mass (KLOE$_{(4)}$). The limits from the A1 [38] and APEX [39] fixed-target experiments; the limits from the ϕ Dalitz decay (KLOE$_{(1)}$) [40,41] and $e^+e^- \to U\gamma$ process where the U boson decays in e^+e^- or $\mu^+\mu^-$ (KLOE$_{(3)}$ and KLOE$_{(2)}$ respectively) [20,21]; the WASA [42], HADES [43], BaBar [44] and NA48/2 [45] limits are also shown. The solid lines are the limits from the muon and electron anomaly [15], respectively. The gray line shows the U boson parameters that could explain the observed a_μ discrepancy with a 2σ error band (gray dashed lines) [15]. (For interpretation of the references to color in this figure, the reader is referred to the web version of this article.)

This includes contributions from kinematic cuts, trigger, tracking, acceptance and PID-likelihood effects. The total systematic error on the global analysis efficiency ranges between 0.7% and 0.4% as $M_{\pi\pi}$ increases.

6. Upper limits

We did not observe any excess of events with respect to the estimated background with significance larger than three standard deviations over the whole M_U explored spectrum. We thus extracted the mass dependent limits on ε^2 at 90% confidence level (CL) by means of the CL_S technique [33]. The procedure requires as inputs the measured invariant mass spectrum, the estimated irreducible total background and the U boson signal for each $M_{\pi\pi}$ bin. The measured spectrum is used as input without any efficiency or background correction. The signal is generated varying the U boson mass hypothesis in steps of 2 MeV. At each step, a Gaussian peak is built with a width corresponding to the invariant mass resolution of the dipion system. The systematic uncertainties were taken into account by performing a Gaussian smearing of the evaluated background according to the estimates in Section 5 and Fig. 6. The results of the statistical procedure are shown in Fig. 8 in terms of the number N_{CLS} of U boson signal events excluded at 90% CL.

We computed the limit on the mixing strength ε^2 by means of the following formula [20,21]:

$$\varepsilon^2 = \frac{\alpha'}{\alpha} = \frac{N_{CLS}}{\epsilon_{eff} \cdot L \cdot H \cdot I}, \quad (1)$$

where ϵ_{eff} is the global analysis efficiency (see Fig. 7), L is the integrated luminosity, H is the radiator function computed at QED NLO corrections with a 0.5% uncertainty [34–37], I is the effective $e^+e^- \to U \to \pi^+\pi^-$ cross section integrated over the single mass bin centered at $M_{\pi\pi} = M_U$ with $\varepsilon = 1$. The uncertainties on H, ϵ_{eff}, L, and I, propagate to the systematic error on ε^2 via eq. (1). The resulting uncertainty on ε^2 is lower than 1% and has been taken into account in the estimated limit. Fig. 9 shows the results from eq. (1) after a smoothing procedure (to make them more readable), compared with limits from other experiments in the mass range 0–1 GeV. Our 90% CL upper limit on ε^2 reaches a maximum value of 1.82×10^{-5} at 529 MeV and a minimum value of 1.93×10^{-7} at 985 MeV. The sensitivity reduction due to the $\omega \to \pi^+\pi^-\pi^0$ decay is of the same order of the statistical fluctuations and thus not visible after the smoothing procedure.

7. Conclusions

We used an integrated luminosity of 1.93 fb^{-1} of KLOE data to search for dark photon hadronic decays in the $e^+e^- \to U\gamma$, $U \to \pi^+\pi^-$ continuum process. No signal has been observed and a limit at 90% CL has been set on the coupling factor ε^2 in the energy range between 527 and 987 MeV. The limit is more stringent than other limits in the ρ–ω region and above.

Acknowledgements

We warmly thank our former KLOE colleagues for the access to the data collected during the KLOE data taking campaign. We thank the DAΦNE team for their efforts in maintaining low background running conditions and their collaboration during all data taking. We want to thank our technical staff: G.F. Fortugno and F. Sborzacchi for their dedication in ensuring efficient operation of the KLOE computing facilities; M. Anelli for his continuous attention to the gas system and detector safety; A. Balla, M. Gatta, G. Corradi and G. Papalino for electronics maintenance; M. Santoni, G. Paoluzzi and R. Rosellini for general detector support; C. Piscitelli for his help during major maintenance periods. This work was supported in part by the EU Integrated Infrastructure Initiative Hadron Physics Project under contract number RII3-CT-2004-506078; by the European Commission under the Seventh Framework Programme through the 'Research Infrastructures' action of the 'Capacities' Programme, Call: FP7-INFRASTRUCTURES-2008-1, Grant Agreement No. 227431; by the Polish National Science Centre through the Grants Nos. 2011/03/N/ST2/02652, 2013/08/M/ST2/00323, 2013/11/B/ST2/04245, 2014/14/E/ST2/00262, 2014/12/S/ST2/00459.

References

[1] F. Zwicky, Helv. Phys. Acta 6 (1933) 110–127;
F. Zwicky, Astrophys. J. 86 (1937) 217.
[2] K. Olive, et al., Review of particle physics, Chin. Phys. C 38 (2014) 090001.
[3] B. Holdom, Phys. Lett. B 166 (1985) 196.
[4] C. Boehm, P. Fayet, Nucl. Phys. B 683 (2004) 219.
[5] P. Fayet, Phys. Rev. D 75 (2007) 115017.
[6] Y. Mambrini, J. Cosmol. Astropart. Phys. 1009 (2010) 022.
[7] M. Pospelov, A. Ritz, M.B. Voloshin, Phys. Lett. B 662 (2008) 53.

[8] O. Adriani, et al., Nature 458 (2009) 607.
[9] P. Jean, et al., Astron. Astrophys. 407 (2003) L55.
[10] J. Chang, et al., Nature 456 (2008) 362.
[11] F. Aharonian, et al., Phys. Rev. Lett. 101 (2008) 261104.
[12] A.A. Abdo, et al., Phys. Rev. Lett. 102 (2009) 181101.
[13] R. Barnabei, et al., Eur. Phys. J. C 56 (2008) 333.
[14] M. Aguilar, et al., AMS Collaboration, Phys. Rev. Lett. 110 (2013) 141102.
[15] M. Pospelov, Phys. Rev. D 80 (2009) 095002.
[16] G.W. Bennett, et al., Muon G-2 Collaboration, Phys. Rev. D 76 (2006) 072003.
[17] R. Essig, P. Schuster, N. Toro, Phys. Rev. D 80 (2009) 015003.
[18] B. Batell, M. Pospelov, A. Ritz, Phys. Rev. D 79 (2009) 115008.
[19] M. Reece, L.T. Wang, J. High Energy Phys. 07 (2009) 051.
[20] A. Anastasi, et al., KLOE-2 Collaboration, Phys. Lett. B 750 (2015) 633.
[21] D. Babusci, et al., KLOE-2 Collaboration, Phys. Lett. B 736 (2014) 459.
[22] M. Adinolfi, et al., Nucl. Instrum. Methods A 488 (2002) 51.
[23] M. Adinolfi, et al., Nucl. Instrum. Methods A 482 (2002) 364.
[24] M. Adinolfi, et al., Nucl. Instrum. Methods A 492 (2002) 134.
[25] L. Barzè, et al., Eur. Phys. J. C 71 (2011) 1680.
[26] H. Czyż, A. Grzelinska, J.H. Kühn, G. Rodrigo, Eur. Phys. J. C 39 (2005) 411.
[27] J.H. Kühn, A. Santamaria, Z. Phys. C 48 (1990) 445.
[28] F. Ambrosino, et al., KLOE Collaboration, Nucl. Instrum. Methods A 534 (2004) 403.
[29] F. Ambrosino, et al., KLOE Collaboration, Phys. Lett. B 670 (2009) 285.
[30] F. Ambrosino, et al., KLOE Collaboration, Phys. Lett. B 700 (2011) 102.
[31] D. Babusci, et al., KLOE-2 Collaboration, Phys. Lett. B 720 (2013) 111.
[32] G. Gounaris, J.J. Sakurai, Phys. Rev. Lett. 21 (1968) 244.
[33] G.C. Feldman, R.D. Cousins, Phys. Rev. D 57 (1998) 3873.
[34] G. Rodrigo, H. Czyż, J.H. Kühn, M. Szopa, Eur. Phys. J. C 24 (2002) 71.
[35] H. Czyż, A. Grzelinska, J.H. Kühn, G. Rodrigo, Eur. Phys. J. C 27 (2003) 563.
[36] H. Czyż, A. Grzelinska, J.H. Kühn, G. Rodrigo, Eur. Phys. J. C 33 (2004) 333.
[37] S. Actis, et al., Working Group on Radiative Corrections and Monte Carlo Generators for Low Energies Collaboration, Eur. Phys. J. C 66 (2010) 585.
[38] H. Merkel, et al., A1 Collaboration, Phys. Rev. Lett. 112 (2014) 221802.
[39] S. Abrahamyan, et al., APEX Collaboration, Phys. Rev. Lett. 107 (2011) 191804.
[40] F. Archilli, et al., KLOE-2 Collaboration, Phys. Lett. B 706 (2012) 251.
[41] D. Babusci, et al., KLOE-2 Collaboration, Phys. Lett. B 720 (2013) 111.
[42] P. Adlarson, et al., WASA-at-COSY Collaboration, Phys. Lett. B 726 (2013) 187.
[43] G. Agakishiev, et al., HADES Collaboration, Phys. Lett. B 731 (2014) 265.
[44] J.P. Lees, et al., BaBar Collaboration, Phys. Rev. Lett. 113 (2014) 201801.
[45] J.R. Batley, et al., NA48/2 Collaboration, Phys. Lett. B 746 (2015) 178.